AIAA JOURNAL
Vol. 39, No. 5, May 2001

Some Modeling Issues on Trailing-Edge Vortex Shedding

Wei Ning*
ALSTOM Power, Lincoln, England LN5 7FD, United Kingdom
and
Li He†
University of Durham, Durham, England DH1 3LE, United Kingdom

A numerical study has been carried out to investigate modeling issues on trailing-edge vortex shedding. The vortex shedding from a circular cylinder and a VKI turbine blade is calculated using a two-dimensional unsteady multiblock Navier–Stokes solver. The unsteady stresses are calculated from the unsteady solutions. The distributions of the unsteady stresses are analyzed and compared for the cylinder case and the cascade case, respectively. The time-averaged equations are then solved, and the effectiveness of the unsteady stresses in suppressing trailing-edge vortex shedding is checked. Finally, the time-independent solution produced by solving the time-averaged equations is compared with the time-averaged solution obtained by integrating the unsteady solutions. The numerical results have demonstrated that a time-independent vortex shedding solution can be achieved by solving the Navier–Stokes equations with the unsteady stresses and the time-averaged effects of the vortex shedding can be included.

Nomenclature

D	=	cylinder or blade trailing-edge circle diameter
l_{mix}	=	mixing length
U	=	vector of unsteady conservative variables
u	=	velocity in axial direction
v	=	velocity in tangential direction
x	=	Cartesian coordinate in axial direction
y	=	Cartesian coordinate in tangential direction
ρ	=	density
$\bar{()}$	=	global mean component
$()'$	=	random fluctuation component
$\tilde{()}$	=	periodic fluctuation component

Introduction

VORTEX shedding is a self-excited unsteady flow phenomenon in turbomachinery blading with a blunt trailing edge. It is known that the formation of vortex streets produces a substantial component of the blade profile loss in gas turbines.[1] Understanding and predicting trailing-edge vortex shedding is of great importance in turbomachinery for further improvement of machine performance.

From the computational point of view, a straightforward way to predict the trailing-edge vortex shedding is to solve the unsteady Navier–Stokes equations. Unfortunately, the very small length scale and high frequency of vortex shedding make the unsteady calculations too expensive for routine design. Several latest efforts on vortex-shedding unsteady calculations[2–4] have shown that even a two-dimensional vortex-shedding unsteady calculation requires a very large amount of CPU time.

As far as a turbomachine designer is concerned, it is highly desirable to obtain a time-independent solution that can include the time-averaged effects of vortex shedding. To this end, solving the time-averaged equations seems to be an attractive approach. The difficulty in doing so is that extra closure models are required to model the unsteady stresses in time-averaged equations. The modeling issues associated with unsteady flows induced by the blade-row interactions and blade oscillation have been addressed by some researchers.[5–8] This paper presents an effort toward modeling the vortex shedding. Before any vortex-shedding model is developed, one issue needs to be addressed first: Can a vortex shedding time-independent solution be achieved by solving the time-averaged Navier–Stokes equations with "unsteady stress" terms? The present work is intended to address this issue by a computational study.

Numerical Methods

The baseline numerical solver in the present work is a multiblock solver.[9] The computational method solves the two-dimensional unsteady Navier–Stokes equations on a multiblock mesh using the four-stage Runge–Kutta time-marching scheme in time and cell-vertex finite volume scheme in space.

The original solver only deals with laminar flows. In the present work a mixing-length turbulence model in a simple form, similar to that adopted by Roberts,[10] is implemented. The turbulent viscosity in this model is given by

$$\mu_t = \rho l_{\text{mix}}^2 |\omega| \tag{1}$$

where

$$|\omega| = \left| \frac{\partial u}{\partial y} - \frac{\partial v}{\partial x} \right|$$

In the near-wall region, the mixing length is given by

$$l_{\text{mix}} = \kappa \min(d_n, d_{\text{lim}}) \tag{2}$$

where κ is the von Kármán constant and is 0.41; d_n is the distance from the solid wall; and d_{lim} is a limiting value of the mixing length, specified by the user. In the wake region the mixing length is taken as κd_{lim}. It is recognized that vortex-shedding unsteady calculations are sensitive to turbulence models.[2,3] In the present work the sensitivity will be examined by simply specifying different d_{lim} values in calculations.

To investigate the modeling issues on vortex shedding, the time-averaged Navier–Stokes equations about the vortex shedding are solved. To obtain the time-averaged equation, the unsteady flow induced by the vortex shedding is decomposed to be a global mean component $\bar{U}$ plus a periodic mean component $\tilde{U}$, which is contributed by periodic vortex shedding, and a random component U', which is contributed by flow turbulence, as

$$U = \bar{U} + \tilde{U} + U' \tag{3}$$

This notation follows a work by Reynolds and Hussain[11] on studying organized waves in turbulent shear flow. The time-averaged equation for the global mean flow can be obtained by substituting expression (3) into the two-dimensional flow governing equations and globally

Received 1 February 2000; revision received 13 July 2000; accepted for publication 13 July 2000.

*Senior Design Engineer, Compressor Group, Industrial Turbine Segment, P.O. Box 1, Waterside South.
†Professor and Chair in Thermodynamics and Fluid Mechanics, School of Engineering.

time averaging them. Because of the nonlinearity of the momentum and energy equations, time averaging will generate extra stress terms, such as $\overline{(\rho\tilde{u})\tilde{v}}$ and $\overline{(\rho u)'v'}$, etc. The $\overline{(\rho u)'v'}$ is the Reynolds stress and is modeled by the mixing-length turbulence model in this work. The stress $\overline{(\rho\tilde{u})\tilde{v}}$ is generated by periodic vortex shedding, and we call it vortex-shedding *unsteady stress.* In this work the random fluctuation and periodic vortex-shedding perturbations are assumed to be uncoupled in a global mean sense, following Reynolds and Hussain.[11]

Comparing the global time-averaged Navier–Stokes equations with the ordinary Reynolds-averaged Navier–Stokes, the only difference is that the vortex shedding unsteady stresses are added in the time-averaged equations. Therefore, the effectiveness of unsteady stresses to suppress vortex shedding can be clearly demonstrated by solving the time-averaged Navier–Stokes equations. In the present work the solution methods for solving the time-averaged equations are the same as that used in the baseline unsteady solver, but the temporal integration of the time-averaged equations should be regarded as in the pseudotime. Because the emphasis of the present work is to investigate the vortex-shedding unsteady stresses, the unsteady stresses in the time-averaged equations are obtained from vortex-shedding unsteady solutions generated by the baseline unsteady solver. For example, the unsteady stress $\overline{(\rho\tilde{u})\tilde{v}}$ can be calculated by

$$\overline{(\rho\tilde{u})\tilde{v}} = \frac{1}{N_P}\sum_{1}^{N_P}(\rho u - \overline{\rho u})(v - \bar{v}) \tag{4}$$

where N_P is the number of time steps in one vortex-shedding period; it can be determined from the vortex-shedding frequency and the size of time step in an unsteady calculation. The time mean variables $\overline{\rho u}$ and $\bar{v}$ are worked out by

$$\overline{\rho u} = \frac{1}{N_P}\sum_{1}^{N_P}\rho u, \qquad \bar{v} = \frac{1}{N_P}\sum_{1}^{N_P} v$$

where ρu and v are instantaneous flow variables obtained from the unsteady calculations.

Unsteady Calculation of Vortex Shedding

The first step of the present work is to calculate trailing-edge vortex shedding by solving the unsteady Navier–Stokes equations using the baseline multiblock solver. The calculations are conducted for flows past a circular cylinder and a VKI turbine cascade. The time-averaged flowfields and vortex-shedding unsteady stresses are calculated from the unsteady solutions, as just described.

Laminar Vortex Shedding Behind a Circular Cylinder

A laminar flow around a cylinder of a diameter D of 0.2 m is calculated at a Reynolds number (based on the cylinder diameter and free stream velocity) of 3×10^3. The calculation is carried out in a domain that is made up of two cylinders. The pitch of the computational domain is set to be $6.5D$ in order to avoid the interference of the vortex shedding between the two cylinders. The computational mesh has four blocks, as shown in Fig. 1. The mesh in the first block, which is around the cylinder, is an O-type mesh with 101×21 points, and the mesh in the other three blocks is a simple H-type mesh.

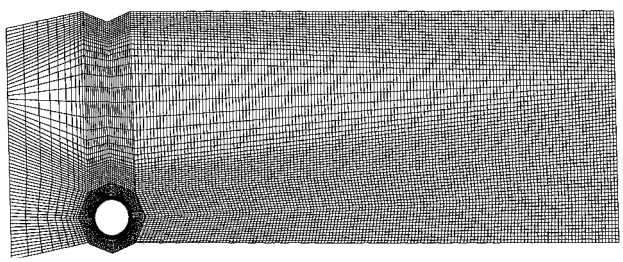

Fig. 1 Computational mesh for circular cylinders.

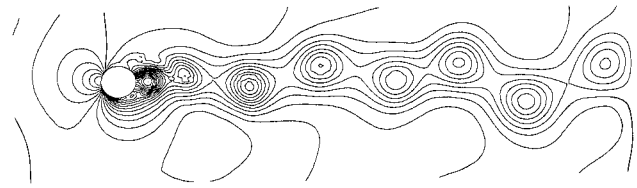

Fig. 2 Instantaneous static-pressure contours.

Fig. 3 Instantaneous entropy contours.

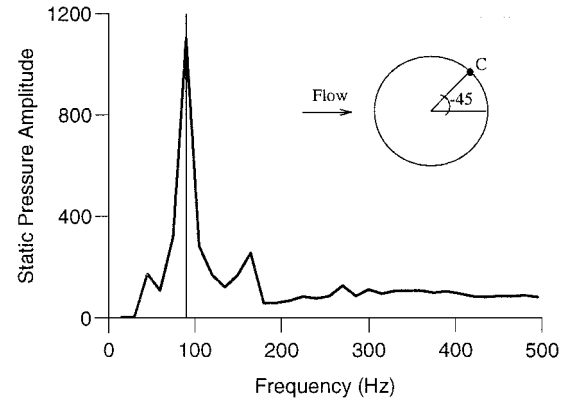

Fig. 4 Static-pressure frequency spectra at point C on cylinder.

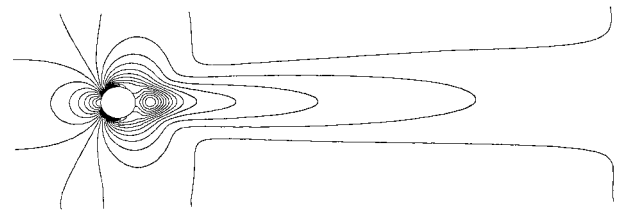

Fig. 5 Time-averaged static-pressure contours from unsteady calculation.

The calculation shows that the unsteady Navier–Stokes equations need to be time marched in about 25 shedding cycles from a one-dimensional initial guess to achieve a periodic vortex shedding. The instantaneous static pressure and entropy contours are presented in Figs. 2 and 3. The static-pressure spectrum near the trailing edge, as shown in Fig. 4, shows that the predicted vortex-shedding frequency is 90 Hz. The result gives a Strouhal number of 0.197 (based on the cylinder diameter and freestream velocity), very close to the empirical value of 0.192.

Once the periodic vortex shedding is achieved, the unsteady solution is time averaged over a shedding period to produce a time-averaged flowfield. The time-averaged static-pressure contours are shown in Fig. 5, and they are symmetric along the wake centerline. Figure 6 presents the time-averaged static-pressure distribution along the cylinder surface and the wake centerline. The time-averaged static pressure in the region of separated flow just downstream of the cylinder (the base region) is lower than that in the freestream. It is known that the lower base pressure is closely related with the loss production associated with vortex shedding.

Based on the instantaneous unsteady solution and the time-averaged solution, the vortex-shedding unsteady stresses are calculated. The contours of three primary unsteady stresses

$[\overline{(\rho\tilde{u})\tilde{u}}, \overline{(\rho\tilde{u})\tilde{v}}, \overline{(\rho\tilde{v})\tilde{v}}]$ are presented in Fig. 7; all of the stresses are nondimensionalized by $\frac{1}{10}$ of the inlet dynamic head $(0.5\rho_{\text{inlet}}u^2_{\text{inlet}})$. The streamwise normal stress $\overline{(\rho\tilde{u})\tilde{u}}$ is symmetric along the wake center, and double peaks appear near the end of the vortex formation region at about x/D of 1.0–1.5 ($x = 0$ corresponds to the center of cylinder). The $\overline{(\rho\tilde{u})\tilde{u}}$ mainly remains bimodal in the wake and makes very little contribution on the wake centerline. The structure of the stress $\overline{(\rho\tilde{u})\tilde{v}}$ is similar to the $\overline{(\rho\tilde{u})\tilde{u}}$ but is antisymmetric along the wake center. The pitchwise normal stress $\overline{(\rho\tilde{v})\tilde{v}}$ has only a single peak on the wake centerline approximately at the end of the vortex formation region. The topologies of these three unsteady stresses in the present laminar vortex shedding are very similar to those produced by an experimental study[12] on a turbulent vortex shedding behind a circular cylinder. The similarity between the laminar and turbulent flows might suggest that the turbulence does not have a strong effect on the main structure of vortex-shedding unsteady stresses.

Vortex Shedding from a VKI Turbine Blade

To investigate trailing-edge vortex shedding for turbomachine blades, a VKI turbine cascade is considered. This VKI turbine blade is a large-scale low-cambered nozzle guide vane. The vortex shedding from this turbine blade has recently been experimentally studied by Cicatelli and Sieverding.[13] This test case has been numerically investigated by Manna and Mulas[2] and Arnone and Pacciani.[3]

A four-block computational mesh is generated in the present investigation. The mesh in the first block, which is around the blades is an O-type mesh with a mesh size of 271 × 35. The mesh in the other three block is an H-type mesh. The four-block mesh has a total of 41,897 points. An enlarged view of the mesh near the blade trailing edge is shown in Fig. 8. In the test the flow has a Reynolds number of 2.5×10^6 and an outlet Mach number of 0.409.

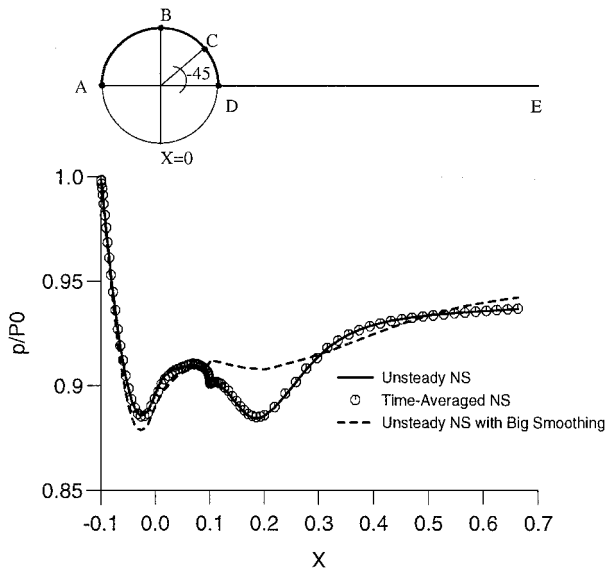

Fig. 6 Static-pressure distribution on cylinder surface and along wake (A-B-C-D-E).

Before the calculation is carried out under the test flow conditions, a low-Reynolds-number laminar vortex-shedding result from the VKI blade is calculated. The purpose is to create a case without any turbulence effects in order to avoid any uncertainties caused by the turbulence modeling. In this laminar case the Reynolds number is specified to be 2.5×10^4, which is two orders of magnitude lower than the test value. After the unsteady solution is time marched about 50 shedding periods, a periodic vortex shedding is achieved. In the calculation each shedding period requires about 1250 time steps and takes about 2280 s CPU time running on a single SGI R10000 processor. The predicted vortex-shedding Strouhal number for this laminar case is 0.235. The instantaneous static pressure and entropy contours are shown in Figs. 9 and 10, indicating a rigorous vortex-shedding street.

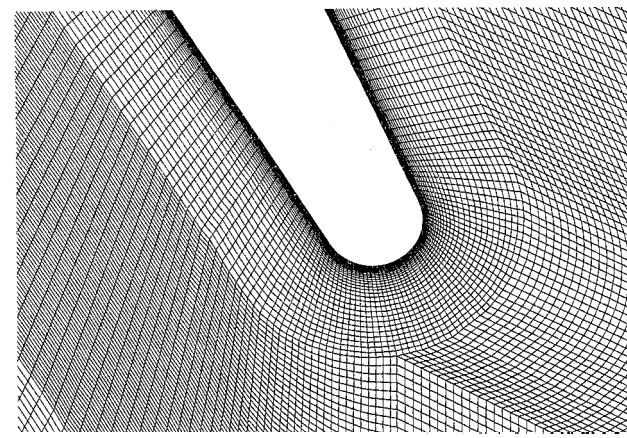

Fig. 8 Enlarged view of mesh around the VKI blade trailing edge.

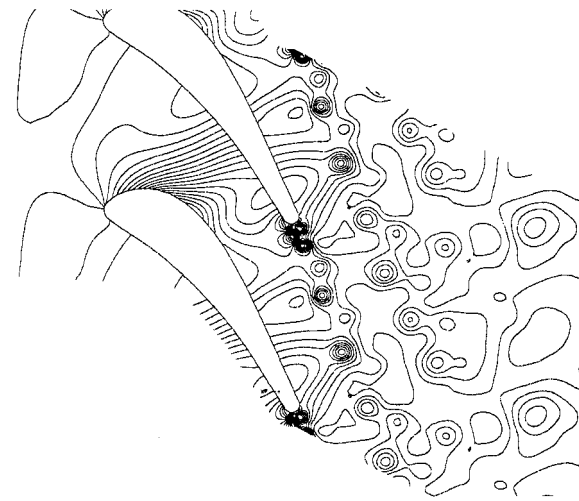

Fig. 9 Instantaneous pressure contours for laminar flow.

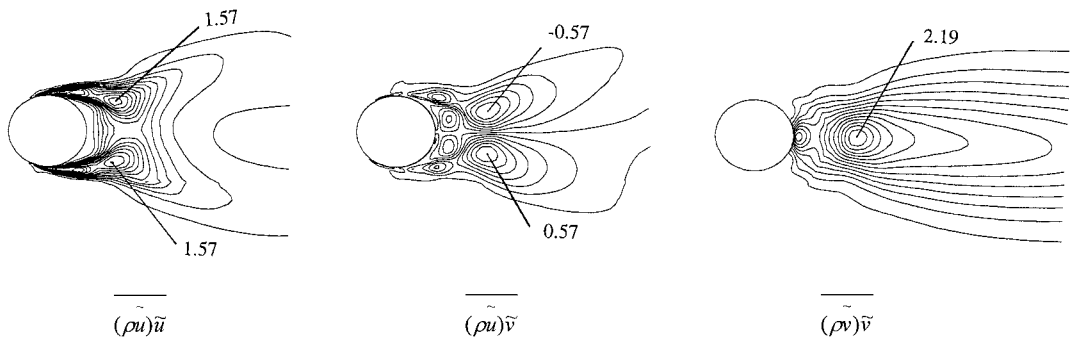

Fig. 7 Contours of vortex-shedding unsteady stresses of circular cylinder.

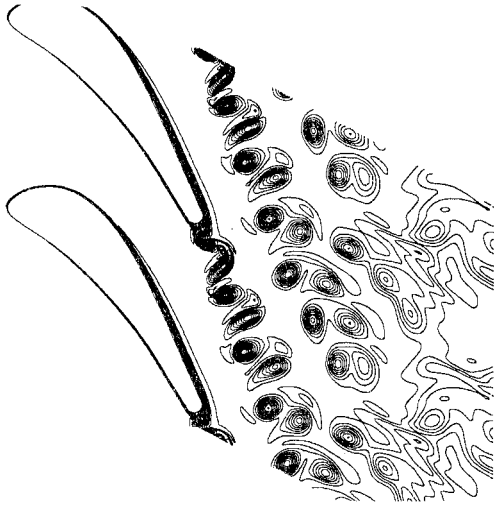

Fig. 10 Instantaneous entropy contours for laminar flow.

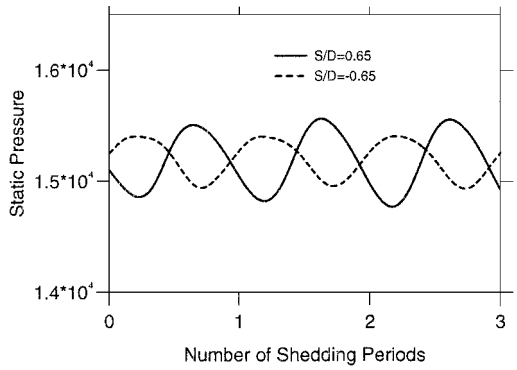

Fig. 11 Static-pressure time traces at points with *S/D* of 0.65 and −0.65.

Then the flow under the test condition is calculated. In the calculation the flow is assumed to be fully turbulent, and the mixing length limit d_{lim} is given to be 2% of the trailing-edge thickness. Numerical tests show that about 60 vortex-shedding periods starting from an initial one-dimensional flow guess are needed to achieve a good level of periodicity. There are about 1200 time steps in one shedding period. Figure 11 presents the static-pressure time traces at points corresponding to abscissa S/D of 0.65 and −0.65 on the blade trailing edge. Here S is the surface length measured from the trailing-edge point, and D is the diameter of the trailing-edge circle. The positive S/D value means the point is on the pressure surface and the negative value is on the suction surface. The pressure fluctuation on the pressure surface is higher than that on the suction surface, which is consistent with the experimental measurement.[13] The static-pressure spectra at point S/D of 0.65 produced by a Fourier transformation are given in Fig. 12. The calculated results give a shedding Strouhal number of 0.245, which is slightly lower than the test value of 0.27. The instantaneous static-pressure and entropy contours are shown in Figs. 13 and 14, and they demonstrate that the turbulent vortex shedding is not as rigorous as the preceding laminar flow case. The time-averaged static pressure around the blade trailing edge is compared with the experimental data in Fig. 15. The base pressure is reasonably predicted by the present calculation. To investigate the sensitivity of the vortex-shedding unsteady calculation to the turbulence model, an unsteady calculation is carried out by specifying the d_{lim} to be 10% of the blade trailing-edge thickness. Numerical tests show that the vortex shedding is suppressed and a steady-state solution is obtained. The predicted base pressure is much higher than the experimental value, as shown in Fig. 15. This calculation confirms the strong dependence of the unsteady vortex-shedding calculation on the turbulence modeling.

Having achieved the periodic vortex shedding, the vortex unsteady stresses for both laminar and turbulent cases are calculated.

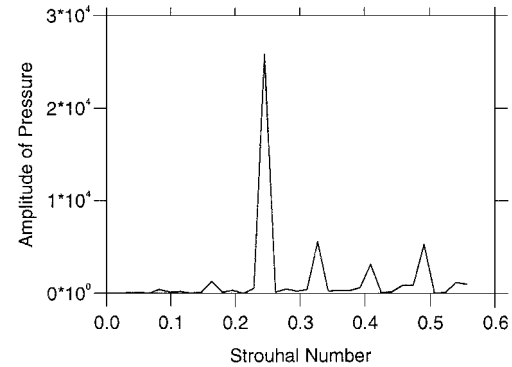

Fig. 12 Static-pressure spectra at point with *S/D* of 0.65.

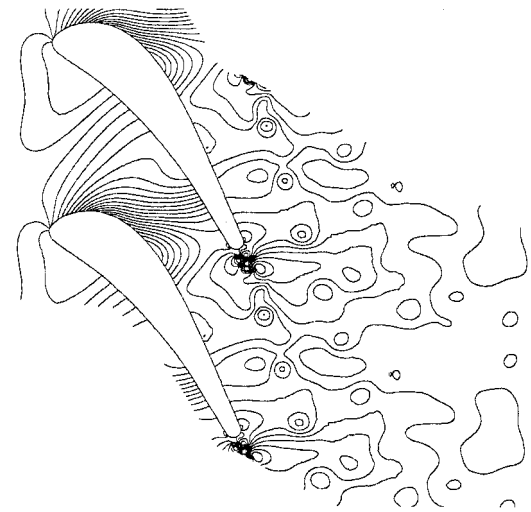

Fig. 13 Instantaneous pressure contours for turbulent flow.

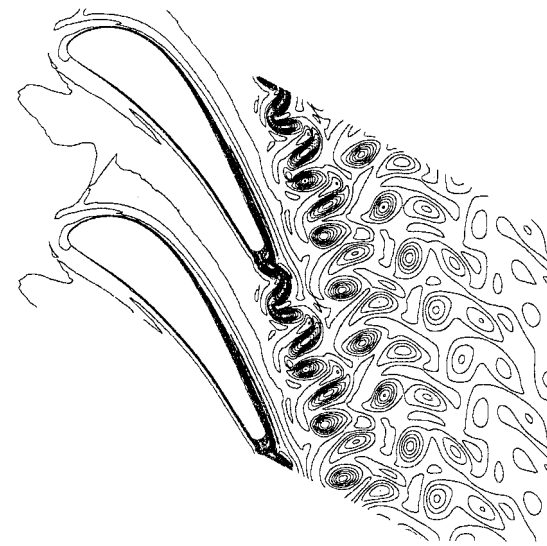

Fig. 14 Instantaneous entropy contours for turbulent flow.

The contours of the unsteady stresses $\overline{(\rho\tilde{u})\tilde{u}}$, $\overline{(\rho\tilde{u})\tilde{v}}$, and $\overline{(\rho\tilde{v})\tilde{v}}$ in the laminar flow case are presented in Fig. 16. The unsteady stress $\overline{(\rho\tilde{u})\tilde{u}}$ is more or less symmetric about the wake centerline. A peak appears about one trailing-edge thickness length downstream of the trailing edge, and it then decays rapidly along the wake. The structure of the stress $\overline{(\rho\tilde{u})\tilde{u}}$ is very similar to the unsteady stress $\overline{(\rho\tilde{v})\tilde{v}}$ in the circular cylinder case as shown in Fig. 7. However, the stress $\overline{(\rho\tilde{u})\tilde{v}}$ is not antisymmetric, and the stress $\overline{(\rho\tilde{v})\tilde{v}}$ is not symmetric along the wake centerline. One reason is that mesh coordinate x in the calculation is not parallel to the wake direction; another

reason is likely to be as a result of the different vortex-shedding intensities from the blade suction and pressure sides. Nevertheless, the topologies of unsteady stresses in the cascade flow are similar to those in the cylinder flow. The contours of the unsteady stresses, $\overline{(\rho\tilde{u})\tilde{u}}$, $\overline{(\rho\tilde{u})\tilde{v}}$, and $\overline{(\rho\tilde{v})\tilde{v}}$ in the turbulent flow case are shown in Fig. 17. The structures of these vortex-shedding unsteady stresses are remarkably similar to the laminar case, but the peak values in the turbulent case are lower because the laminar vortex shedding is more rigorous. Again, all the unsteady stresses presented in Figs. 16 and 17 are nondimensionalized by $\frac{1}{10}$ of the inlet dynamic head.

Solutions of Time-Averaged Equations

The vortex-shedding unsteady stresses in the time-averaged equations are obtained from the preceding unsteady calculations. In the calculations for the time-averaged equations, the computational mesh, flow conditions, time-step size, and artificial smoothing coefficients are all kept the same as their unsteady counterparts. The only difference is that the vortex-shedding unsteady stresses are included.

Circular Cylinder

The calculation residual history, as presented in Fig. 18, shows that a time-independent solution is achieved by solving the time-averaged equations. The static-pressure contours are shown in Fig. 19, and they illustrate that vortex shedding is completely suppressed by the inclusion of the vortex-shedding unsteady stresses. The calculated static-pressure distribution along the cylinder surface and the wake centerline is in very good agreement with the time-averaged one produced by the unsteady calculation, as shown in Fig. 6.

It is recognized that the vortex shedding can be suppressed in different ways, such as excessive artificial damping, very big time steps, etc. In this work a calculation is carried out by solving the unsteady Navier–Stokes equation with an excessive artificial smoothing coefficient. The calculation residual history is also plotted in Fig. 18, and it suggests that the vortex shedding is suppressed and a steady-state solution is obtained. However, the comparison between the steady static-pressure distribution with the time-averaged one in Fig. 6 shows that the large variation of the static-pressure in the base region is missed when suppressing the vortex shedding by using the excessive artificial smoothing.

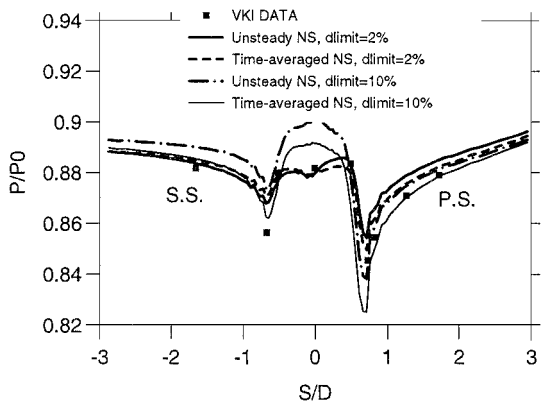

Fig. 15 Static-pressure distribution around blade trailing edge.

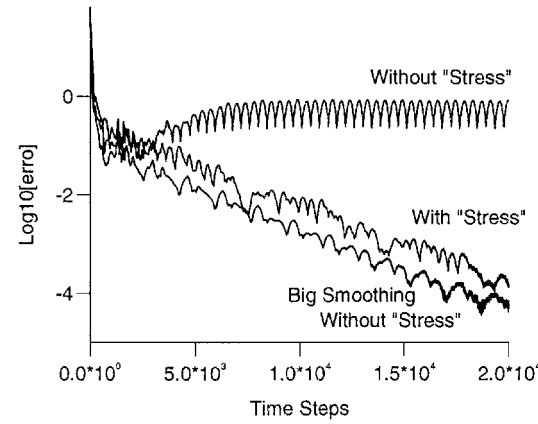

Fig. 18 Calculation residual history for circular cylinder flow.

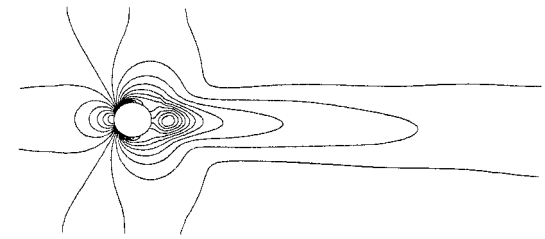

Fig. 19 Static-pressure contour by solving NS with unsteady stresses for circular cylinder flow.

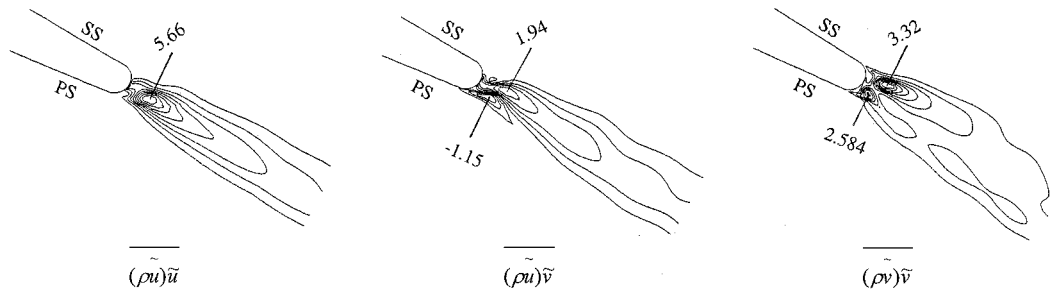

Fig. 16 Contours of vortex-shedding unsteady stresses for laminar cascade flow.

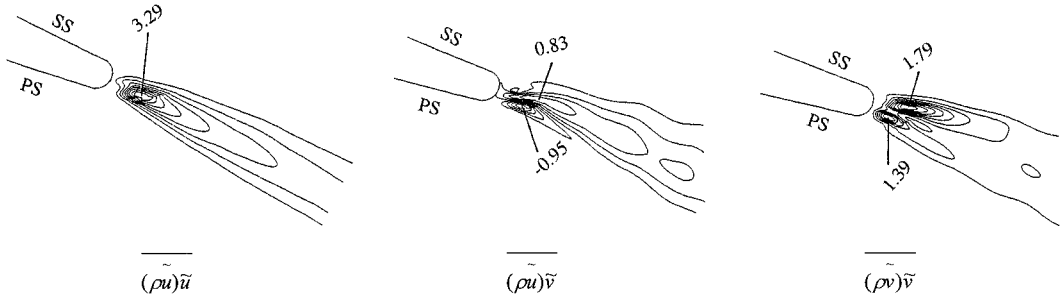

Fig. 17 Contours of vortex-shedding unsteady stresses for turbulent cascade flow.

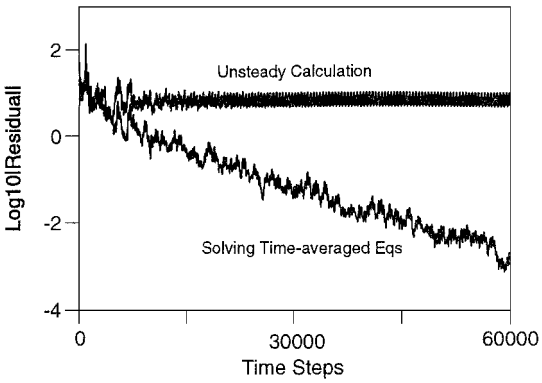

Fig. 20 Calculation residual history for cascade laminar flow.

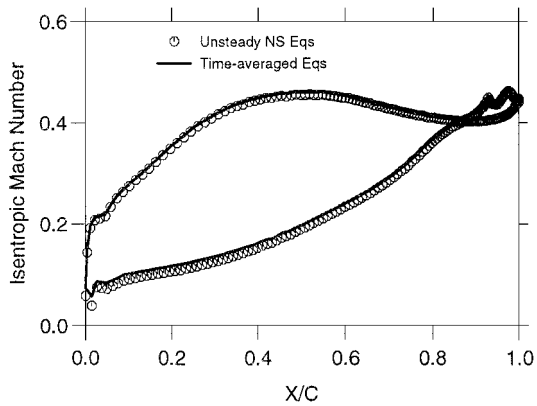

Fig. 21 Isentropic Mach-number distribution on the blade surface for laminar flow.

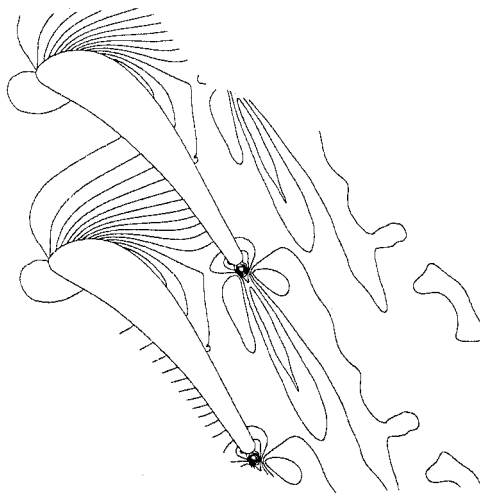

Fig. 22 Static-pressure contours by solving Navier–Stokes with unsteady stresses for laminar flow.

VKI Turbine Blade

The effectiveness of vortex-shedding unsteady stresses to suppress the vortex shedding is then investigated on the VKI turbine blade case. The first attempt is made on the low-Reynolds-number laminar flow case. The residual history of solving the time-averaged equations with the stress terms is shown in Fig. 20, and it shows that a time-independent solution is achieved. The steady-state isentropic Mach-number distribution on the blade surface compares very well with the time-averaged results produced by the unsteady calculation, as shown in Fig. 21. The static-pressure contours, as presented in Fig. 22, show no sign of vortex shedding.

Then a similar attempt is made for the turbulent flow case. The calculation of solving the time-averaged equations shows that the vortex shedding is suppressed, and a time-independent solution can be achieved. The static-pressure contours (Fig. 23) produced by the time-averaged equations are very similar to the time-averaged static-pressure contours generated by the unsteady calculation (Fig. 24). The base pressure around the blade trailing edge obtained by solving the time-averaged equations agrees well with the time-averaged pressure as presented in Fig. 15.

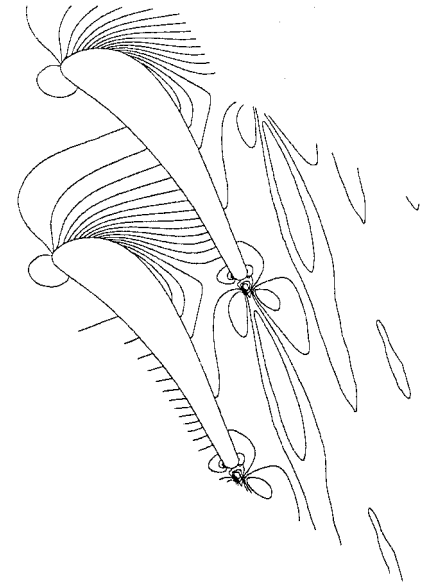

Fig. 23 Time-averaged static-pressure contours by solving unsteady Navier–Stokes for turbulent flow.

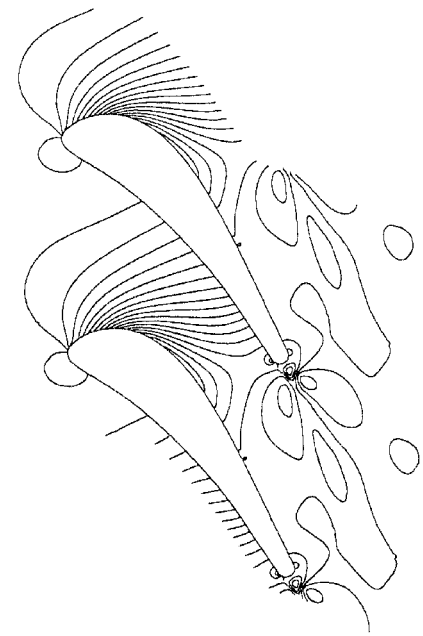

Fig. 24 Static-pressure contours by solving Navier–Stokes with unsteady stresses for turbulent flow.

To investigate the turbulence modeling dependence of the time-independent solutions, a calculation is then carried out to solve the time-averaged equations by specifying the d_{lim} to be 10% of the trailing-edge thickness. This calculation still uses the unsteady stresses obtained in the unsteady calculation with the d_{lim} of 2% of the trailing-edge thickness. Again a time-independent flowfield is obtained, and the base pressure is plotted in Fig. 15 as well. The base pressure calculated by the time-averaged equations gives a better agreement with the VKI data than the pure unsteady calculation when d_{lim} is specified as 10% of the trailing-edge thickness. This result implies that the time-averaged equations exhibit less dependence on turbulence modeling than the vortex-shedding unsteady calculations.

Conclusions

The results of the present computational study suggest the following:

1) To achieve a vortex-shedding time-independent solution by solving Navier–Stokes equations with vortex-shedding unsteady stresses is possible. The resultant time-independent solution can adequately include the vortex-shedding time-averaged effects.

2) The structures of the vortex-shedding unsteady stresses are fairly simple. The similarity of the unsteady stresses between the circular cylinder flow and the cascade flow suggests that the development of the vortex-shedding modeling in turbomachinery could benefit from the detailed studies on vortex shedding behind circular cylinders.

3) Vortex-shedding characteristics are sensitive to artificial damping and turbulence modeling. Steady-state solutions without unsteady stresses can significantly change the base pressure and therefore the blade profile loss. Some preliminary numerical results suggest that solving the time-averaged equations might have a smaller dependence on turbulence models.

Given the feasibility of directly computing the time-averaged effect of vortex shedding by including the vortex-shedding stress terms, further efforts in the unsteady stress modeling should be made in the future.

Acknowledgments

This study is part of the Ph.D. work of the first author, sponsored by ALSTOM Power, which was carried out at the School of Engineering, University of Durham. Additional financial support was provided by an ORS award to the first author. The authors wish to acknowledge R. G. Wells and Y. S. Li for their technical support.

References

[1]Denton, J. D., "Loss Mechanisms in Turbomachines," the 1993 IGTI Scholar Lecture, *Journal of Turbomachinery*, Vol. 115, No. 4, 1993, pp. 621–656.

[2]Manna, M., and Mulas, M., "Navier–Stokes Analysis of Trailing Edge Induced Unsteady Flow in a Turbine Blade," VKI Lecture Series 1994-06, von Kármán Inst. for Fluid Dynamics, May 1994.

[3]Arnone, A., and Pacciani, R., "Numerical Prediction of Trailing Edge Vortex Shedding," American Society of Mechanical Engineers, Paper 97-GT-89, June 1997.

[4]Sondak, D. L., and Dorney, D. J., "Simulation of Vortex Shedding in a Turbine Stage," American Society of Mechanical Engineers, Paper 98-GT-242, June 1998.

[5]Adamczyk, J. J., "Model Equations for Simulating Flows in Multistage Turbomachinery," American Society of Mechanical Engineers, Paper 85-GT-226, June 1985.

[6]Giles, M. B., "An Approach for Multi-Stage Calculations Incorporating Unsteadiness," American Society of Mechanical Engineers, Paper 92-GT-282, 1992.

[7]He, L., "I. Modeling Issues for Computation of Unsteady Turbomachinery Flows," VKI Lecture Series 1996-05, von Kármán Inst. for Fluid Dynamics, 1996.

[8]Ning, W., and He, L., "Computation of Unsteady Flows around Oscillating Blades Using Linear and Nonlinear Harmonic Euler Methods," *Journal of Turbomachinery*, Vol. 120, No. 3, 1998, pp. 508–514.

[9]He, L., "A Multiple-Zone N-S Solver," User's Manual, School of Engineering, Univ. of Durham, Durham, England, U.K., May 1996.

[10]Roberts, Q. D. H., "The Trailing Edge Loss of Subsonic Turbine Blades," Ph.D. Dissertation, Dept. of Engineering, Univ. of Cambridge, Cambridge, England, U.K., Dec. 1997.

[11]Reynolds, W. C., and Hussain, A. K. M. F., "The Mechanics of an Organised Wave in Turbulent Shear Flow, Part 3, Theoretical Models and Comparisons with Experiments," *Journal of Fluid Mechanics*, Vol. 54, Pt. 2, July 1972, pp. 263–288.

[12]Cantwell, B., and Coles, D., "An Experimental Study of Entrainment and Transport in the Turbulent near Wake of a Circular Cylinder," *Journal of Fluid Mechanics*, Vol. 136, Pt. 2, Nov. 1983, pp. 321–374.

[13]Cicatelli, G., and Sieverding, C. H., "The Effect of Vortex Shedding on the Unsteady Pressure Distribution Around the Trailing Edge of a Turbine Blade," American Society of Mechanical Engineers, Paper 96-GT-39, June 1996.

P. Givi
Associate Editor